

## Raman study of temperature dependence of lattice modes in calcite

A K SOOD, A K ARORA, V UMADEVI and G VENKATARAMAN  
Reactor Research Centre, Kalpakkam 603 102, India

MS received 8 September 1980

**Abstract.** The temperature dependence of the line width and the peak position of the  $E_g$  librational mode (of nominal frequency  $285\text{ cm}^{-1}$ ) and the  $E_g$  translational mode (of nominal frequency  $155\text{ cm}^{-1}$ ) in calcite ( $\text{CaCO}_3$ ) have been studied by laser-Raman spectrometry. The role of orientational relaxation as a possible process contributing to the line width has been evaluated. It is concluded that reorientations do not play a major part in relation to the present observations. It is further shown that the latter can be understood on the basis of cubic and quartic anharmonic processes. The data also suggest that certain phonon interactions earlier considered insignificant for peak shift in calcite, do contribute significantly.

**Keywords.** Laser Raman spectroscopy; external modes; librations; calcite; anharmonicity; line widths; temperature dependence; lattice modes.

### 1. Introduction

Calcite ( $\text{CaCO}_3$ ) has been the subject of varied spectroscopic investigations in the past (Porto *et al* 1966 and references therein; Park 1966, 1967 and Sakurai and Sato 1971). From the work of Porto *et al* it has emerged that (i) the Raman spectrum is fully consistent with the selection rules based on the point group symmetry of the crystal, and (ii) there is no anomalous depolarisation of the  $A_{1g}$  internal mode of the carbonate ion as was reported by earlier workers. Park, and Sakurai and Sato have concentrated on the anharmonic aspects of the vibrations, and have reported the temperature-dependence of the vibrational parameters for several modes. The present work is of a similar nature, and addresses itself to a study of the temperature dependence of two low-frequency Raman-active external modes not covered in earlier studies, namely  $E_g$  ( $\sim 285\text{ cm}^{-1}$ ) and  $E_g$  ( $\sim 155\text{ cm}^{-1}$ ). These modes are associated predominantly with the librational and centre of mass motions respectively of the carbonate ion (see figure 1), and the aim was to see if the line shapes of these modes were in any way influenced by orientational relaxations of the  $\text{CO}_3^{2-}$  ion. It has emerged from our studies that reorientations do not play an important role in relation to line shapes, and that the latter are determined by anharmonicity associated with multiphonon processes.

The plan of the paper is as follows: In § 2 we present briefly the experimental details. The processing of the data and the extraction of the line shape parameters are considered in § 3 wherein the results are also presented. § 4 which constitutes the main body of the paper is devoted to a discussion of the results. § 5 contains some concluding remarks.

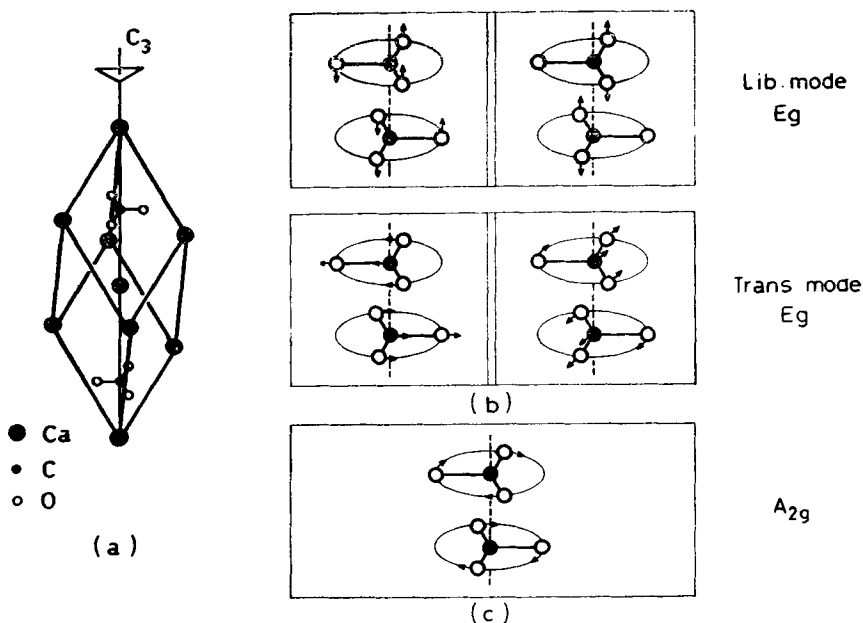


Figure 1. (a) Unit cell of calcite. (b) Vibrational patterns for the Raman active vibrational and translational modes studied in the present work. (c) The  $A_{2g}$  vibrational mode. The large amplitude version of this would tend towards angular re-orientation.

## 2. Experimental

The samples used (size  $10 \times 5 \times 5$  mm) were obtained by cleaving naturally occurring single crystals parallel to the rhombohedral face. The Raman spectra were recorded in a laser-Raman spectrometer built around a model 14018 SPEX double monochromator. The laser employed was a 30 mW He-Ne laser. Detection of the scattered light was done using a cooled ITT-FW130 photomultiplier tube, followed by a photon-counting system. The laser, the collection optics, the cooling arrangement for the detector and the photon-counting system were all locally built. The dark current achieved was  $\sim 2.5$  CPS.

Measurements were made in the range 100-710 K. In the range 100-300 K, the sample was mounted in a glass cryostat using liquid nitrogen as the refrigerant. An electric heater on the cold finger of the cryostat was used to achieve the desired intermediate temperatures. A small furnace was used to go beyond room temperature. The constancy of the sample temperature was within  $\pm 1$  K, and the absolute accuracy of temperatures quoted is estimated as  $\pm 3$  K.

All the spectra recorded were unpolarised. A slit-width of roughly  $4 \text{ cm}^{-1}$  (in terms of FWHM of the resolution function) was employed throughout. Preliminary scans were made in the analogue mode, *i.e.*, by using a rate meter followed by an x-y recorder. The spectra recorded for detailed analysis were however obtained digitally, with counts sampled at each wave number for about 100 sec, to give an ordinate accuracy of  $\sim 1\%$  in the wings.

### 3. Results

Figures 2a and 2b show typical spectra at different temperatures. It is evident that as temperature increases, the lines broaden significantly. The intensity in the wings also increases, possibly due to multiphonon processes. By smoothly interpolating between the two wings, the one-phonon part of the spectrum can be (approximately) isolated and examined further.

We see from figure 2 that the lines have typical resonance shapes, broadened of course by instrumental resolution. Accordingly, we assume that the unmodified line is described by

$$I(\omega) = \frac{1}{\pi} \frac{\Gamma}{(\omega - \omega_0)^2 + \Gamma^2} [1 + n(\omega)]. \quad (1)$$

Here  $\omega_0$  is the resonance frequency, and  $\Gamma$  the half-width at half maximum. The quantity  $1 + n(\omega)$  with

$$n(\omega) = [\exp(\hbar \omega / k_B T) - 1]^{-1},$$

describes the population factor.

Now the slit width, though small, produces a measurable contribution to the broadening. Therefore,  $\Gamma$  cannot be directly read off from the measured spectra. As a prelude to making resolution corrections, we determined the resolution function in the following way: We first scattered the He-Ne laser beam off a piece of cardboard and recorded the spectrum of the scattered beam using the same slit width as employed in the Raman measurements. The natural line width of the laser beam being very small ( $\sim 1$  MHz), the observed line profile corresponds entirely to the instrument resolution function at the laser beam frequency, *i.e.*,  $15802 \text{ cm}^{-1}$ . We then recorded the neon plasma line at  $15665 \text{ cm}^{-1}$  (this corresponds to a Raman shift of  $137 \text{ cm}^{-1}$ ) using once again the same slit width. Here too, the natural width ( $\sim 500$  MHz) was much smaller than the slit width employed. As expected, both profiles were reasonably consistent with a Gaussian shape, *i.e.*,

$$R(\omega - \omega_c) = (a/\pi)^{1/2} \exp[-a(\omega - \omega_c)^2], \quad (2)$$

where  $\omega_c$  is the centre frequency and  $a$  the resolution parameter. The values of  $a$  for both the lines were found to be the same within experimental error. We have therefore assumed that the resolution function is the same over the entire observed range of frequencies, and further is given by (2).

When a Lorentzian is folded with (2), the modified line shape is described by

$$I_m(\omega) = \frac{1}{\pi} \text{Re} [(\pi a)^{1/2} e^{ap^2} \text{erfc}(pa^{1/2})], \quad (3)$$

where  $p = \Gamma - i(\omega - \omega_0)$ ,

and  $\text{erfc}$  denotes the complimentary error function. Ideally, we should have fitted our data to (3) (with, of course, correction for the population factor and the base line)

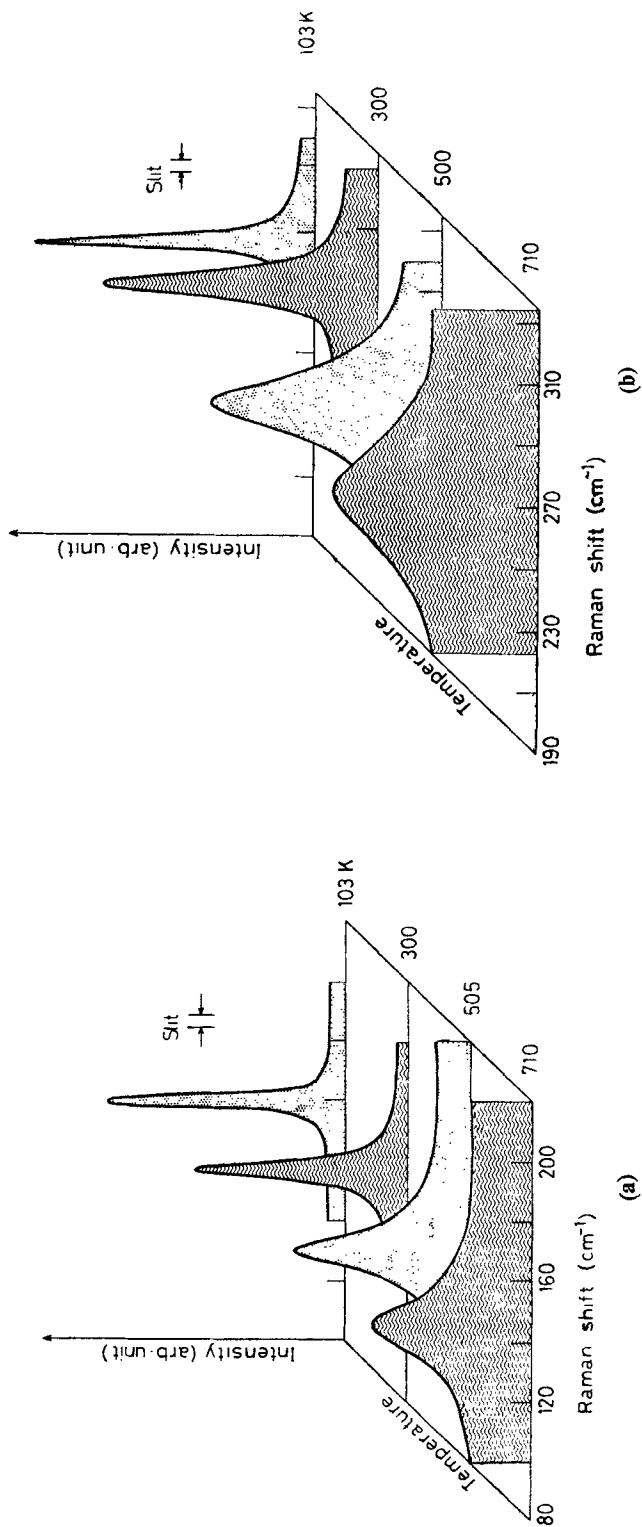


**Figure 2.** Raman spectra for the translational mode (2a) and librational mode (2b). For convenience of presentation smooth lines have been drawn through the data points. The slit width employed is also shown.

for extracting  $\Gamma$  and  $\omega_0$ . Owing to the excessive computing time required to do this, we adopted a somewhat simpler procedure. We first computed  $I_m(\omega)$  for various assumed values of  $\Gamma$  with  $\omega_0$  fixed at some arbitrary value. Using this set of computed modified spectra, we then established a curve of  $\Gamma_m$  (half-width of the modified spectrum) versus  $\Gamma$ . With this curve available, the  $\Gamma$  appropriate to any measured spectrum can be read off, treating the observed width  $\Gamma_{\text{obs}}$  as equal to  $\Gamma_m$ . For obtaining  $\Gamma_{\text{obs}}$ , we first corrected the observed readings for the population factor. A graphical procedure was then employed to deduce  $\Gamma_{\text{obs}}$  using which  $\Gamma$  was obtained as described above.

Besides treating the data graphically, we have also used a computer to extract  $\Gamma_{\text{obs}}$  and  $\omega_0$ . For this, the observed points after correction for the population factor were least-squares fitted to:

$$I_{\text{obs}}(\omega) = A_1 + A_2(\omega - \omega_m) + A_3 \frac{\Gamma_{\text{obs}}}{(\omega - \omega_0)^2 + \Gamma_{\text{obs}}^2}. \quad (4)$$

Here  $\omega_m$  is the lowest Raman shift in the experiment. The quantities  $A_1$ ,  $A_2$ ,  $A_3$ ,  $\omega_0$  and  $\Gamma_{\text{obs}}$  are adjustable parameters. Implicit in the use of the form (4) is the assumption that resolution does not modify the *functional form* of the line shape but merely 'fattens' the Lorentzian, a not unreasonable assumption when  $\Gamma a^{1/2} \gg 1$ .

The values of  $\omega_0$  obtained by graphical analysis were in good accord with those deduced *via* (4). The results of the computer-aided analysis had a slightly greater precision and were the ones finally adopted. As regards  $\Gamma_{\text{obs}}$ , both methods gave very similar values for the high-temperature data, but, for low temperatures, the computer fit was of a slightly poorer quality. This is to be expected since the shape fitted to is a Lorentzian whereas the shape emerging from experiment has a strong Gaussian admixture, being resolution-dominated to some extent. The values of  $\Gamma_{\text{obs}}$  we finally relied upon were essentially those obtained by the graphical analysis. We should add that besides yielding values for  $\omega_0$ , the computer analysis served the added purpose of assessing the errors in the deduced quantities.

Figure 3 shows the line width as a function of temperature deduced *via* above analysis, and figure 4 shows the temperature dependence of the resonant frequencies.

## 4. Discussion

### 4.1 Line width

The carbonate ion in calcite is a well-bound unit, as is evident from the high values of the internal mode frequencies. It is common for such well-bound molecular groups to exhibit reorientations, and our aim, as already indicated, was to see if such reorientation processes contributed to the line width of the vibrational mode, as happens for example, in several ammonium salts.

Now the width  $\Gamma$  arises essentially due to the interruption of the vibrations by various physical processes. As in the case of nuclear resonances, one may suppose that each of these processes makes an independent contribution to the width, so that

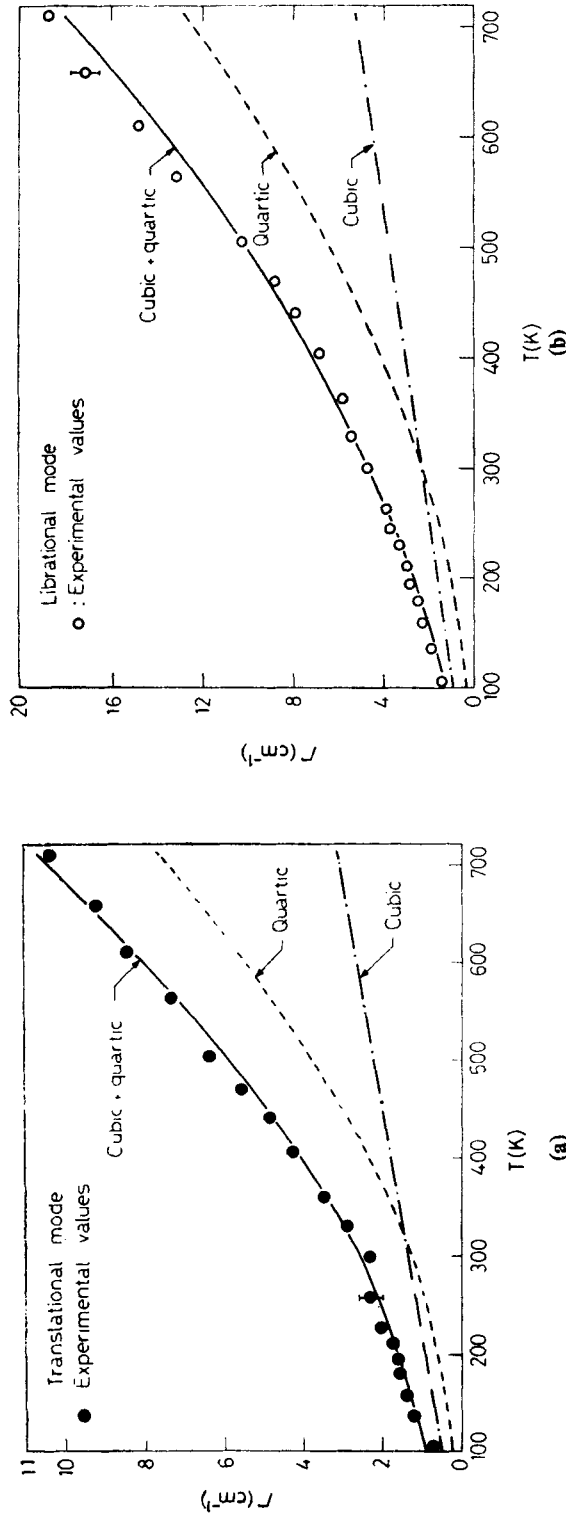


Figure 3. Temperature dependence of the linewidth after correction for resolution effects as discussed in the text for translational mode (3a) and librational mode (3b). The lines show theoretical calculations based on (7), (8) and (13). The parameters of the fit are given in table 2.

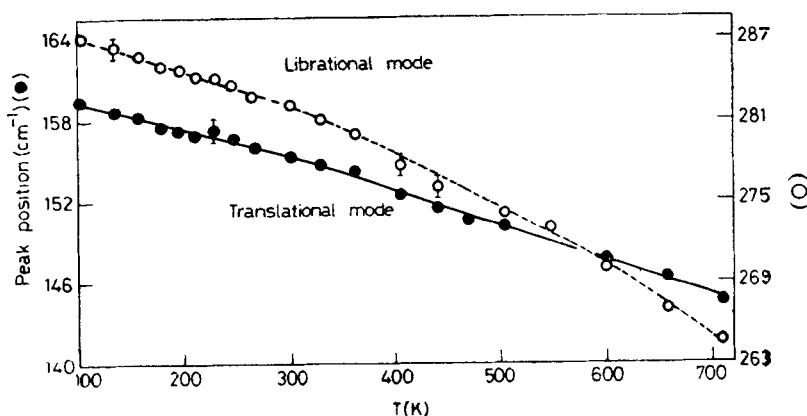


Figure 4. Variation of the vibrational frequency with temperature.

we may set  $\Gamma = \sum_i \Gamma_i$  where the index  $i$  runs over all the processes involved. In our case, we would expect  $i$  to include reorientations and the usual cubic and quartic anharmonic processes. For analysing the data, we need explicit expressions for  $\Gamma_{\text{reorient}}$ ,  $\Gamma_{\text{cubic}}$  and  $\Gamma_{\text{quartic}}$ .

At this stage, we would like to clarify what we mean by reorientations in the present context. This is done in figure 5. The oxygen atoms of the  $\text{CO}_3^{2-}$  ion move in a potential well with three-fold angular symmetry as shown. Angular jumps occur randomly taking the ion from one configuration to an equivalent one, where it resumes all its normal vibrations over again. The phase interruptions to the vibration make a contribution  $\Gamma_{\text{reorient}}$  to the width (Rakov 1964; Sood *et al* 1978). An illuminating analysis of the effect of phase interruptions on the width of a resonance line has been given by Ben Reuven (1969) within a harmonic oscillator model. It turns out that the quantity  $\Gamma_{\text{reorient}}$  may be taken to have the form

$$\Gamma_{\text{reorient}} = \nu_0 \exp(-U/k_B T), \quad (5)$$

where  $U$  is the activation energy and  $\nu_0$  the usual prefactor.

As regards the anharmonic contribution, *i.e.*, that due to multiphonon processes, formal analyses are available in many papers (e.g. Maradudin and Fein 1962; Cowley 1963, 1968; Klemens 1966; Wallis *et al* 1966, and Ipatova *et al* 1967). Many-body techniques are used, and in effect the problem reduces to the calculation of the proper self energy (denoted usually by the symbol  $\Sigma$  but represented by  $G$  by Maradudin and Fein). Diagrams contributing to  $\Sigma$  are shown in figure 6. In passing we remark that in the early work of Maradudin and Fein (1962), only contributions to 0 ( $\lambda^2$ ) were considered *i.e.*, those from diagrams in figures 6a and 6c. Subsequently, Ipatova *et al* (1967) took account of contributions from diagrams in figures 6b and 6d. It is pertinent also to add that the diagram in figure 6e was not considered in earlier work since it gives a zero contribution for Bravais crystals and for non-primitive crystals in which every atom is at a centre of inversion (Maradudin and Fein 1962). This however does not apply to calcite; it turns out that the contribution is of the same functional form as that arising from figure 6c but of a much smaller magnitude.

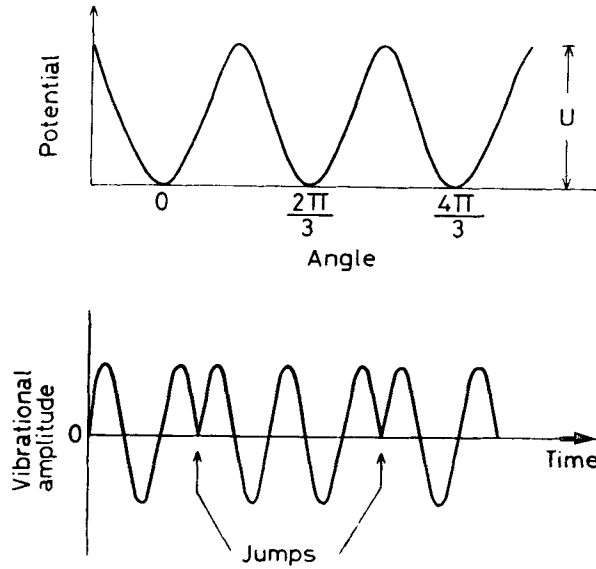


Figure 5. (a) Schematic drawing of the three-fold potential. (b) Illustrating the interruption to a normal mode of vibration caused by the reorientation process. Such interruptions can make a contribution to the line width as given by (5).

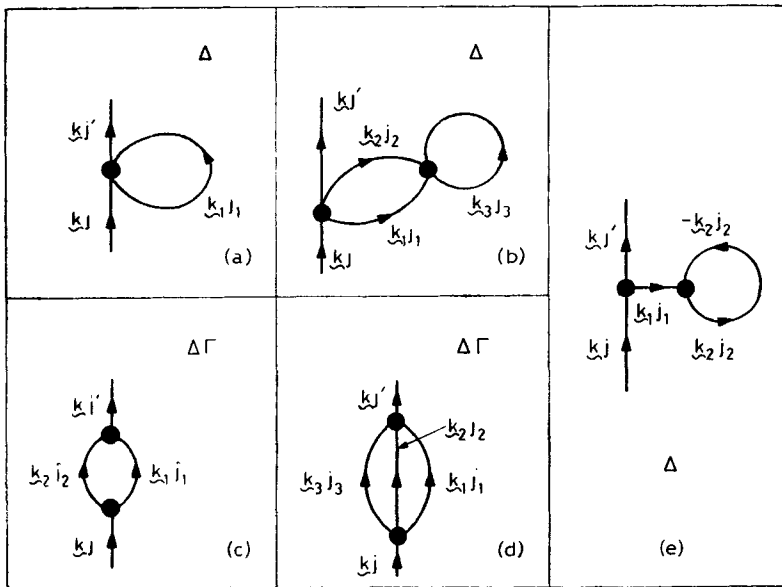


Figure 6. Diagrams contributing to the proper self energy. The insets show whether the diagram contribute to peak shift ( $\Delta$ ) alone or peak shift and line width ( $\Gamma$ ).

The quantities of experimental interest, namely the line width function  $\Gamma$  and the frequency shift function  $\Delta\omega$  are obtained from the relation (Maradudin and Fein 1962).

$$\lim_{\delta \rightarrow 0^+} -\frac{1}{k_B T} \sum (kj; \omega \pm i\delta) = \Delta\omega(kj; \omega) \mp i\Gamma(kj; \omega), \quad (6)$$

where  $\mathbf{k}$  denotes the phonon wave vector and  $j$  the branch index.

Presently, we direct attention to  $\Gamma$ . The formal expressions are quite forbidding, and rule out the possibility of explicit evaluation, especially for a crystal of the complexity of calcite. Accordingly, we resort to a phenomenological formula which, however, is based on the formal result both in spirit and in content. Thus, guided by Park (1966, 1967) we suppose that cubic anharmonicity leads to the decay of a phonon of frequency  $\omega_0$  into two phonons each of frequency  $(\omega_0/2)$ , which then results in an expression of the form.

$$\Gamma_{\text{cubic}} = A \left\{ [\exp(\hbar \omega_0/2 k_B T) - 1]^{-1} + \frac{1}{2} \right\}, \quad (7)$$

where  $A$  is a constant. Similarly, for the quartic process, we may suppose that  $\omega_0$  decays into three other phonons each of frequency  $(\omega_0/3)$  which then gives (Sakurai and Sato 1971)

$$\Gamma_{\text{quartic}} = B \left\{ [(\exp(\hbar \omega_0/3 k_B T) - 1)^{-1} + \frac{1}{2}]^2 + \frac{1}{12} \right\}, \quad (8)$$

where  $B$  is a constant. It is worth noting that in the high-temperature limit,

$$\Gamma_{\text{cubic}} \sim T \text{ and } \Gamma_{\text{quartic}} \sim T^2.$$

Turning now to our data, our first attempt was to fit the corrected widths assuming

$$\Gamma = \Gamma_{\text{reorient}} + \Gamma_{\text{cubic}}, \quad (9)$$

the individual contributions being as in (5) and (7). In writing (9) it is assumed that the quartic process is not as significant as reorientations. A fairly good fit to the data could be made with parameters as in table 1. In making the fit, the values assumed for  $\omega_0$  were  $285 \text{ cm}^{-1}$  and  $156 \text{ cm}^{-1}$  for the librational and translational modes respectively. Now if the fit is meaningful, then the value deduced for the activation energy must be in reasonable accord with an independent estimate. One way of

Table 1. Fit to model in (9) with parameters as in (5) and (7).

	$\nu_0$ ( $\text{cm}^{-1}$ )	$U$ (kcal/mole)	$A$ ( $\text{cm}^{-1}$ )	Remarks
Librational mode	$110 \pm 13$	$3.39 \pm 0.15$	$2.63 \pm 0.06$	
Translational mode	$58 \pm 5$	3.39	$0.84 \pm 0.04$	$U$ was fixed to be 3.39 kcal/mole
Translational mode	$43 \pm 5$	$2.96 \pm 0.15$	$0.84 \pm 0.04$	$U$ was also an adjustable parameter

obtaining the latter is to consider the dynamics of the  $\text{CO}_3^{2-}$  ion in the three-fold potential well. The Schrödinger equation is

$$-\frac{\hbar^2}{2I} \frac{d^2 \Psi}{d\alpha^2} + \frac{V_0}{2}(1 - \cos 3\alpha) \Psi = E \Psi, \quad (10)$$

where  $I$  is the moment of inertia about the  $C_3$ -axis and  $E$  the eigenvalue. The librational frequency  $\nu$  is identified as usual with the frequency difference between the lowest and the next higher eigenvalues. By a suitable transformation (see, for example, Venkataraman *et al* 1966), the Schrödinger equation is readily cast in the form of Mathieu's equation from which we get

$$V_0 \text{ (cal/mole)} = 0.0114 \nu^2 I^*, \quad (11)$$

where  $\nu$  is expressed in  $\text{cm}^{-1}$  and  $I^* = 10^{40} \times I$  ( $\text{g cm}^2$ ). It is to be noted that librations here refer to the mode  $A_{2g}$  illustrated in figure 1, and have a frequency  $\sim 165 \text{ cm}^{-1}$  (Plihal 1973). Using this value for  $\nu$  and taking  $I^* = 124.5$ , we deduce

$$V_0 \sim 38.6 \text{ k cal/mole}, \quad (12)$$

which clearly is very much higher than the activation energy emerging from the fit discussed earlier. If instead of reorientations about the  $C_3$  axis we consider a rotation of  $\pi$  about the  $x$ -axis, we obtain  $V_0 = 1.603 \nu^2 \text{ cal/mole}$ . The librational mode now pertinent is the  $R_x$  mode of frequency  $285 \text{ cm}^{-1}$  which then leads to  $V_0 = 130.2 \text{ k cal/mole}$ , a value much higher than that in (12). We believe (12) is more representative of the barrier and therefore conclude that the fit achieved is not physically significant. It is obvious that had we inserted the value (12) as an estimate for  $U$  in (5), we would directly have inferred that reorientations would not make significant contributions to the observed width. However, we approached the data without bias to see what emerged. The exercise is not without value since, on occasion, width data is directly fitted to a reorientation model (Wang and Wright 1973). The present experience shows clearly the need for caution.

Having ruled out reorientations as a contributing factor to the width, we now analyse the latter in terms of anharmonic processes alone, taking

$$\Gamma = \Gamma_{\text{cubic}} + \Gamma_{\text{quartic}}, \quad (13)$$

with the individual contributions as given by (7) and (8). The fit achieved is shown in figure 3, and the relevant parameters are summarised in table 2. Attention is drawn

Table 2. Fit to the model in (13) with parameters as in (7) and (8).

	$A \text{ (cm}^{-1}\text{)}$	$B \text{ (cm}^{-1}\text{)}$
Librational mode	$1.50 \pm 0.07$	$0.46 \pm 0.002$
Translational mode	$0.50 \pm 0.03$	$0.08 \pm 0.004$

to the fact that  $(B/A) \sim 0.16$  for the translational mode and  $= 0.71$  for the librational mode. This is not unexpected since dissipation of vibrational energy *via* a four-phonon process will be more important for a mode of higher frequency.

#### 4.2 Frequency shift

We now turn to the temperature-induced frequency shift of the vibrational modes. As is well known, part of the observed shift can be understood in terms of thermal expansion and the resulting change of (the harmonic) force constants. This is the so-called quasi-harmonic contribution. The remaining part arises due to relaxational processes which, in our case, we attribute (as already explained) to cubic and quartic anharmonicity.

Let  $\omega_0(T)$  denote the frequency of the mode under consideration at temperature  $T$ . In terms of the various shifts mentioned above (Leibfried 1965),

$$\omega_0(T) = \omega_0(0) + \Delta\omega_{\text{qh}}(T) + \Delta\omega_{\text{ah}}(T), \quad (14)$$

where  $\omega_0(0)$  is the frequency at  $0^\circ$  K, and  $\Delta\omega_{\text{qh}}$  and  $\Delta\omega_{\text{ah}}$  are the quasi-harmonic and anharmonic contributions respectively to the shift. Our aim now is to extract  $\Delta\omega_{\text{ah}}$  from the experimental data and then subject it to analysis.

The first step in the above process is to estimate  $\Delta\omega_{\text{qh}}(T)$ . This is possible from a consideration of the Grüneisen constant  $G$  which is related to the manner in which the frequency changes with volume (consequent to expansion). Following Born and Huang (1954) we write

$$\omega_0(T) = \omega_0(0) \exp\left(-\int_0^T G(T') \alpha_V(T') dT'\right). \quad (15)$$

Here  $\alpha_V$  is the volume expansion coefficient. In our experiments, the lowest temperature attained was 103 K. We therefore approximate (15) as

$$\Delta\omega_{\text{qh}}(T) \sim \omega_0(103) \exp\left(-\int_{103}^T G(T) \alpha_V(T) dt\right). \quad (16)$$

As far as the mode frequency is concerned, we estimate from figure 3 that the error made in replacing  $\omega_0(0)$  by  $\omega_0(103)$  is about a few percent. We similarly believe that it is reasonable to neglect the contribution to the integral from 0 K to 103 K. For a uniaxial crystal like calcite,

$$\alpha_V = \alpha_{\parallel} + 2\alpha_{\perp}, \quad (17)$$

where  $\alpha_{\parallel}$  and  $\alpha_{\perp}$  are the expansion coefficients parallel and perpendicular to the unique axis of the crystal.

Rao *et al* (1968) have studied the expansion of calcite between 300 K and 700 K and represent their results *via* the equations

$$\begin{aligned} \alpha_{\parallel} &= 24.670 \times 10^{-6} + 1.74 \times 10^{-8} t - 5.141 \times 10^{-12} t^2, \\ \alpha_{\perp} &= -3.660 \times 10^{-6} - 7.112 \times 10^{-10} t - 3.339 \times 10^{-12} t^2, \end{aligned} \quad (18)$$

where  $t$  is the temperature in degree centigrade.

Below 300 K, information about  $\alpha_V$  is scant, and the only data we have come across is an old one due to Adenstat (1936). This author gives data points for  $\alpha_V$  from 300 K downwards. Unfortunately, at 300 K where the measurements of Adenstat and of Rao *et al* overlap, the absolute values of  $\alpha_V$  do not quite match. However, a smooth curve drawn through the data of Adenstat when spliced to the curve of Rao *et al*, appears quite continuous. Such a composite curve, may therefore well be representative of thermal expansion over the entire temperature range of present interest. Accordingly, we have made a fit to the data of Adenstat, obtaining for the functional form,

$$\alpha_V = (16.99 + 0.027 t - 2.853 \times 10^{-4} t^2) \times 10^{-6}, \quad (19)$$

where, as in (18),  $t$  is the temperature in degree centigrade. The composite curve obtained by combining (18) and (19) over the temperature of present interest is shown in figure 7. It may be noted that this matching procedure essentially implies a vertical shift of the data points of Adenstat by roughly two units on the scale of figure 7.

The Grüneisen constant  $G$  was calculated from the relation

$$G = (\alpha_V V_m / \chi C_V), \quad (20)$$

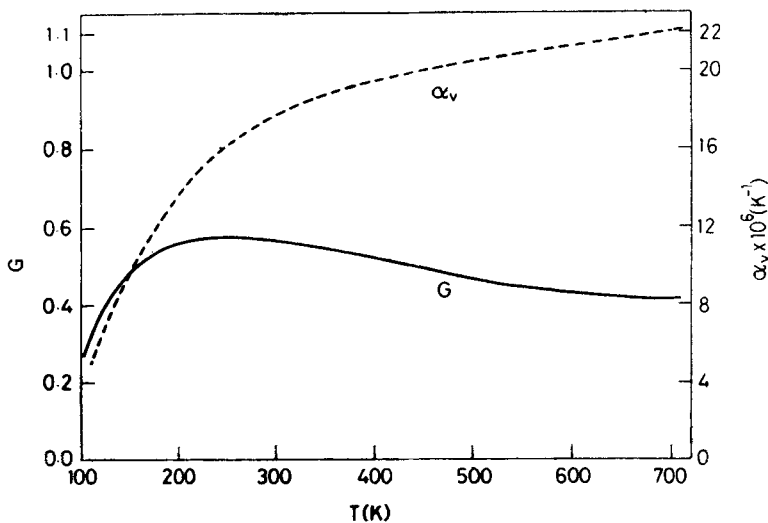


Figure 7. Temperature variation of  $\alpha_V$  and the Grüneisen constant.

where  $V_m$  = molar volume (=34.2 cm<sup>3</sup> for calcite),  $\chi$  is the compressibility and  $C_V$  the specific heat at constant volume. The values of  $\chi$  for  $T > 300$  K were taken from Dandekar (1968); values below room temperature were obtained from this data by extrapolation. Specific heat data were taken from the work of Plihal (1973).

The temperature variation of  $G$  as calculated above is shown in figure 7. The quasi-harmonic shifts computed using this data are shown in figure 8. With all this information available, (14) can now be used to extract  $\Delta\omega_{ah}$ . In doing so, we have made the approximation  $\omega_0(T) - \omega_0(0) \simeq \omega_0(T) - \omega_0(103)$ , as in (16). The shifts thus obtained for the two modes are shown in figure 9.

It now remains to explain the magnitude and trend of these shifts. Ipatova *et al* (1967) have shown (see also Sakurai and Sato 1971), that  $\Delta\omega_{ah}$  can be written as

$$\Delta\omega_{ah}(T) = \Delta\omega'(T) + \Delta\omega''(T), \tag{21}$$

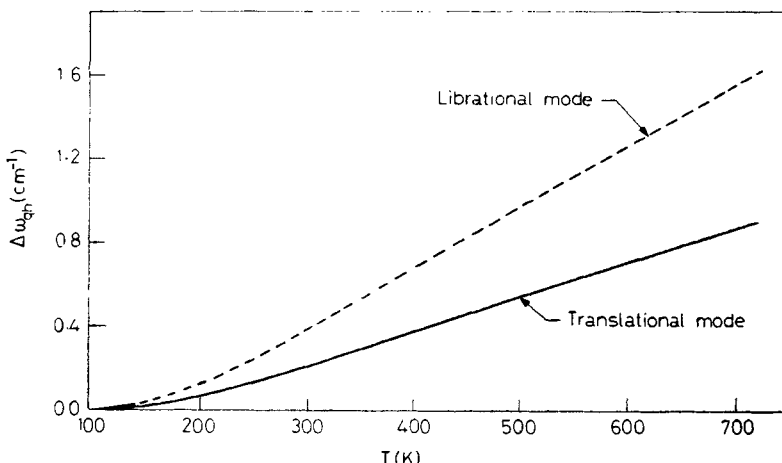


Figure 8. Quasi-harmonic shift estimated as discussed in the text.

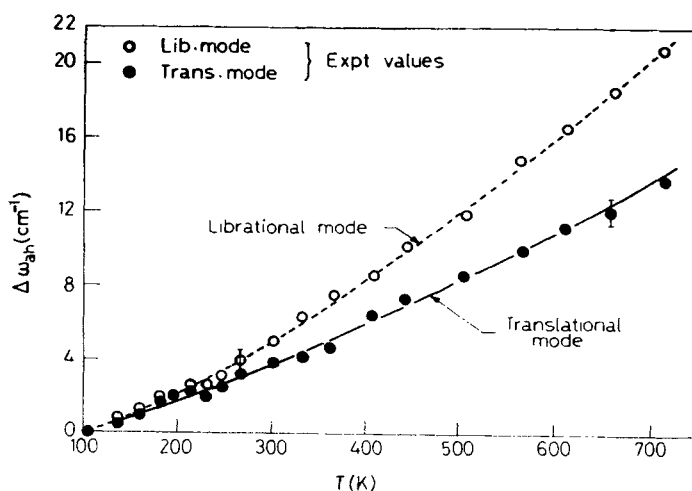


Figure 9. The points denote anharmonic shifts estimated from our data in conjunction with those of figure 8. The solid lines indicate shifts based on (23).

where  $\Delta\omega'$  and  $\Delta\omega''$  are the frequency-independent and frequency dependent contributions. Using an approximate model as earlier for the phonon decay, one has (Sakurai and Sato 1971),

$$\Delta\omega'(T) = C' [\{\exp(\hbar\omega_0/2k_B T) - 1\}^{-1} + \frac{1}{2}] - D' \left[ \left\{ (\exp(\hbar\omega_0/3k_B T) - 1)^{-1} + \frac{1}{2} \right\}^2 + \frac{1}{12} \right], \quad (22a)$$

$$\Delta\omega''(T) = -C'' [\{\exp(\hbar\omega_0/2k_B T) - 1\}^{-1} + \frac{1}{2}] - D'' \left[ \left\{ (\exp(\hbar\omega_0/3k_B T) - 1)^{-1} + \frac{1}{2} \right\}^2 + \frac{1}{12} \right], \quad (22b)$$

where  $C'$ ,  $C''$ ,  $D'$  and  $D''$  are all positive constants. Referring back to figure 6, the two diagrams contributing to  $\Delta\omega'$  are (a) and (b), and lead respectively to the terms with coefficients  $C'$  and  $D'$ . Similarly, diagrams associated with terms in (22b) above are those in (c) and (d). Experiment does not permit a separate determination of the frequency-independent and frequency-dependent parts. Accordingly, we combine the two expressions in (22) into

$$-\Delta\omega_{\text{ah}}(T) = E [\{\exp(\hbar\omega_0/2k_B T) - 1\}^{-1} + \frac{1}{2}] + F \left[ \left\{ (\exp(\hbar\omega_0/3k_B T) - 1)^{-1} + \frac{1}{2} \right\}^2 + \frac{1}{12} \right] + H, \quad (23)$$

where  $E = (C'' - C')$  and  $F = (D' + D'')$ . The constant

$$H = - [(C'' - C')/2 + (D' + D'')/3] \text{ ensures } \Delta\omega_{\text{ah}}(0) = 0.$$

We have fitted our results for the anharmonic shifts to this equation with values for the various parameters as given in table 3. The quality of the fit may be assessed from figure 9.

Sakurai and Sato (1971) have carried out a similar analysis for the IR-active modes  $E_{u(3)}$  (305  $\text{cm}^{-1}$ ),  $A_{2u(a)}$  (886  $\text{cm}^{-1}$ ), and  $E_{u(b)}$  (1416  $\text{cm}^{-1}$ ). Their data are for 300 K and above, in which range, terms in (22) with coefficients  $C'$  and  $C''$  do not contribute much. Sakurai and Sato further argue that the frequency-independent contribution alone is important, so that  $\Delta\omega_{\text{ah}} \sim \Delta\omega'$ . Their arguments do not appear to be convincing to us. In our case, terms with coefficients  $C'$  and  $C''$  are not

**Table 3.** Fit to the model in (23).

	$E$ ( $\text{cm}^{-1}$ )	$F$ ( $\text{cm}^{-1}$ )	$H$ ( $\text{cm}^{-1}$ )
Librational mode	$4.30 \pm 0.30$	$0.34 \pm 0.04$	$-3.1 \pm 0.3$
Translational mode	$1.77 \pm 0.17$	$0.05 \pm 0.01$	$-1.8 \pm 0.2$

negligible as is evident from the non-zero value of  $E$ . (cf. equation (2b) and table 3). Further since  $E > 0$ , it implies  $C' > C''$  which in turn means that the contribution from the frequency-dependent processes outweigh those from the frequency-independent processes. Our findings in this respect are at variance with those of Sakurai and Sato, although it is to be admitted that the modes they have studied are different from those we have.

Finally, we note that as in the case of the line width, the ratio of the contributions from the quartic to the cubic terms i.e.  $(F/E)$  is greater for the librational mode than that for the translational mode.

## 5. Concluding remarks

Our experiments have shown that reorientations do not contribute significantly to the phonon line widths in calcite, unlike the case of many other complex crystals. Of course, this is not to say that reorientations do not occur in calcite. What transpires is that they are not rapid enough to make an impact on the line shape. This in turn is a consequence of the somewhat large barrier heights, as compared to ammonium salts, for example. We have also demonstrated that it is risky to merely fit width data to a reorientation model without counterchecks. It is possible, of course, that some other activation process other than reorientation is present. In the case of calcite we do not conceive of such a possibility and we therefore attribute the observed width entirely to multiphonon processes. Using this approach, the observed data can be reasonably well explained on the basis of simplified models for cubic and quartic anharmonic processes. Further, the frequency shift data strongly indicate that certain processes, namely those associated with diagrams (6c) and (6d) (which were earlier considered to be insignificant for the peak shift in calcite) do contribute to this quantity.

## Acknowledgements

One of us (AKS) would like to acknowledge helpful discussions with Drs S Dattagupta and V Balakrishnan.

## References

- Adenstedt H 1936 *Ann. Phys.* **26** 69
- Ben Reuven A 1969 in *Advances in atomic and molecular physics* Vol 5, ed. D R Bates and I Emstermann (New York: Academic Press)
- Born M and Huang K 1954 *Dynamical theory of crystal lattices* (Oxford: Oxford Univ. Press)
- Cowley R A 1963 *Adv. Phys.* **12** 421
- Cowley R A 1968 *Rep. Prog. Phys.* **31** 123
- Dandekar D P 1968 *J. Appl. Phys.* **39** 3694
- Ipatova I P, Maradudin A A and Wallis R F 1967 *Phys. Rev.* **155** 882
- Klemens P G 1966 *Phys. Rev.* **148** 845
- Leibfried G 1965 *J. Phys. Chem. Sol. Supp.* **1** 237
- Maradudin A A and Fein A E 1962 *Phys. Rev.* **128** 2589
- Park K 1966 *Phys. Lett.* **22** 39

- Park K 1967 *Phys. Lett.* **A25** 490  
Plihal M 1973 *Phys. Status Solidi* **B56** 494  
Porto S P S, Giordmaine J A and Damen T C 1966 *Phys. Rev.* **147** 608  
Rakov A V 1964 as cited in *Raman spectra of molecules and crystals* by M M Sushchinskii, (New York: Israel Programme for Scientific Translation), page 328  
Rao K V K, Naidu S V N and Murthy K S 1968 *J. Phys. Chem. Sol.* **29** 245  
Sakurai T and Sato T 1971 *Phys. Rev.* **B4** 583  
Sood A K, Arora A K, Umadevi V, Datagupta S and Venkataraman G 1978 in *Proc. Sixth Int. Conf. Raman Spect.* Vol. 2, ed E D Schmidt *et al* (London: Heyden), p. 216  
Wallis R F, Ipatova I P and Maradudin A A 1966 *Sov. Phys. Solid State* **8** 850  
Wang C H and Wright R B 1973 *J. Chem. Phys.* **58** 2934  
Venkataraman G, Usha Deniz K, Iyengar P K, Roy A P and Vijayaraghavan P R 1966 *J. Phys. Chem. Sol.* **27** 1103